Title

Tau Internalization is Regulated by 6-O Sulfation on Heparan Sulfate Proteoglycans (HSPGs).

Journal

Scientific reports, 8(1)

ISSN

2045-2322

Authors

Rauch, Jennifer N
Chen, John J
Sorum, Alexander W
et al.

Publication Date

2018-04-01

DOI

10.1038/s41598-018-24904-z

Peer reviewed

SCIENTIFIC REPORTS

OPEN

Tau Internalization is Regulated by 6-O Sulfation on Heparan Sulfate Proteoglycans (HSPGs)

Received: 8 June 2017
Accepted: 28 March 2018
Published online: 23 April 2018

Jennifer N. Rauch[1], John J. Chen[2], Alexander W. Sorum[3], Gregory M. Miller[3], Tal Sharf[1], Stephanie K. See[2], Linda C. Hsieh-Wilson[3], Martin Kampmann[2] & Kenneth S. Kosik[1]

The misfolding and accumulation of tau protein into intracellular aggregates known as neurofibrillary tangles is a pathological hallmark of neurodegenerative diseases such as Alzheimer's disease. However, while tau propagation is a known marker for disease progression, exactly how tau propagates from one cell to another and what mechanisms govern this spread are still unclear. Here, we report that cellular internalization of tau is regulated by quaternary structure and have developed a cellular assay to screen for genetic modulators of tau uptake. Using CRISPRi technology we have tested 3200 genes for their ability to regulate tau entry and identified enzymes in the heparan sulfate proteoglycan biosynthetic pathway as key regulators. We show that 6-*O*-sulfation is critical for tau-heparan sulfate interactions and that this modification regulates uptake in human central nervous system cell lines, iPS-derived neurons, and mouse brain slice culture. Together, these results suggest novel strategies to halt tau transmission.

The Microtubule-Associated Protein Tau (MAPT or tau) is an intrinsically disordered protein that under pathological conditions aggregates into filamentous inclusions known as neurofibrillary tangles (NFTs)[1]. While the composition and structure of NFTs are well characterized[2,3], the *in vivo* process of aggregation is not well understood. The presence of NFTs is characteristic of a number of human diseases, collectively termed tauopathies. In tauopathies, such as Alzheimer's disease (AD), NFT pathology advances in a predictable pattern throughout the brain affecting regions involved in learning and memory[4]. This progression of NFT pathology correlates with cognitive decline in patients and permits neuropathological diagnoses of patients in different stages of AD[5].

The spread of protein aggregates during disease progression is a common theme in many neurodegenerative diseases, including α-synuclein in Parkinson's disease[6], Huntingtin protein in Huntington's disease[7], and superoxide dismutase-1 in amyotrophic lateral sclerosis[8]. However, the exact mechanisms underlying intercellular spread of these aggregates, including tau, is unclear. Increasing evidence suggests the transmission of tau pathology is mediated by the release, uptake, and trafficking of pathogenic or misfolded tau aggregates within synaptically connected neurons[9,10]. Once internalized, misfolded tau proteins act as a seed that recruits soluble endogenous tau into growing aggregates[11]. Aggregated tau is proteotoxic in model systems, suggesting that oligomeric and/or fibrillar tau may contribute to neurodegeneration[12]. However, it is unclear how the different quaternary architectures of tau affect internalization and if all structures have the ability to transfer between neurons. Conflicting studies have shown varying results regarding tau uptake with some studies showing internalization of small monomeric or oligomeric tau species[13] and others suggesting that only oligomeric and/or fibrillized tau is internalized[14]. Discrepancies between culture systems and sources of tau protein may account for these differences, but this has not been explicitly tested. Further, a better understanding of the cellular processes that are necessary for transmission of tau aggregates could lead to the discovery of novel therapeutic strategies that would inhibit the spread of tau pathology and its consequences. Recent work on α-synuclein has shown that a cell surface receptor, lymphocyte activation gene-3 (LAG3), can bind α-synuclein and trigger its endocytosis into neurons[15]. Based on this, and previous observations in the literature[16], we hypothesized that perhaps a receptor could also exist for tau.

[1]Neuroscience Research Institute, Department of Molecular Cellular Developmental Biology, University of California, Santa Barbara, CA, 93106, USA. [2]Institute for Neurodegenerative Diseases, Department of Biochemistry & Biophysics, The California Institute for Quantitative Biomedical Research, Quantitative Biosciences Institute, University of California, San Francisco, and Chan Zuckerberg Biohub, San Francisco, CA, 94158, USA. [3]Division of Chemistry and Chemical Engineering, California Institute of Technology, Pasadena, CA, 91125, USA. Correspondence and requests for materials should be addressed to K.S.K. (email: kenneth.kosik@lifesci.ucsb.edu)

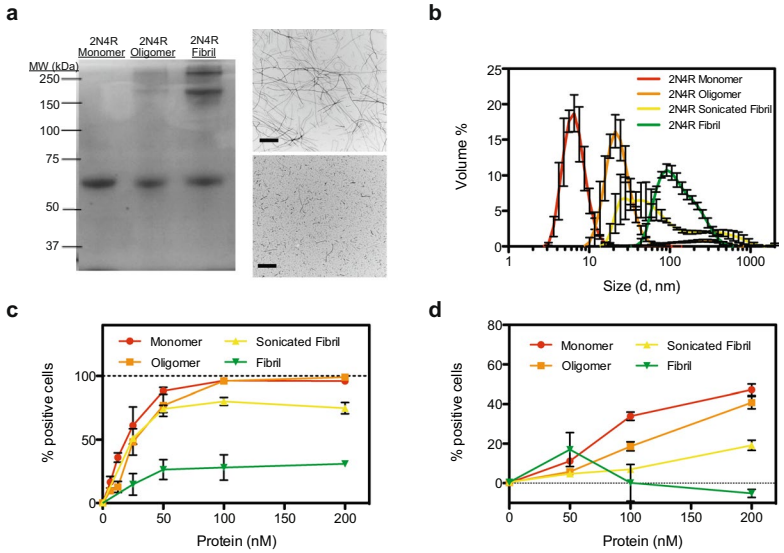

Figure 1. Tau uptake is regulated by quaternary structure. (**a**) 2N4R monomer, oligomer, and fibrillized proteins show distinct banding patterns on a non-reducing SDS-PAGE gel. 2N4R Fibrils before (top) and after (bottom) sonication as visualized by negative-stain EM. Bar represents 500 nm (**b**) DLS of 2N4R monomer, oligomer, fibril, and sonicated fibril species. Experiments were performed in triplicate and the error shown is SD. (**c**) Uptake of 2N4R quaternary structures in H4 cells after 1 h at 37 °C. (**d**) Uptake of 2N4R quaternary structures in iPS-derived neurons after 1 h at 37 °C. For all uptake experiments, three independent experiments were performed in duplicate, identical control experiments were performed at 4 °C and subtracted from 37 °C data to generate final curves shown, and the error shown is SEM.

Heparan sulfate proteoglycans (HSPGs) are a diverse family of proteins modified with the linear sulfated glycosaminoglycan (GAG) heparan sulfate (HS). HSPGs are present in virtually all cells and are involved in a multitude of processes including cell attachment, migration, differentiation, and inflammation[17]. HS chains consists of a basic disaccharide building block β-1,4-linked D-glucuronic acid (GlcA) and α-1,4-linked *N*-acetyl-D-glucosamine (GlcNAc). During assembly, HS chains can be highly modified; GlcNAc residues can be *N*-deacetylated and *N*-sulfated, GlcA can be epimerized at C5 to L-iduronic acid (IdoA), and ester-linked sulfate groups can be installed at C2 of the GlcA/IdoA and/or at C6/C3 of the GlcNAc. There is no defined template for HS modification on HSPGs. Thus, the availability of precursor material and abundance of biosynthetic enzymes in the cell are thought to dictate chain length, sulfation pattern, and epimerization[18]. Previous work has implicated HSPGs as a potential receptor for tau internalization[14,16]. However, this work has not examined whether specific HSPG proteins or specific HS modifications on these proteins can act as determinants for cellular tau entry, and therefore does not contain the molecular detail that would guide therapeutic strategies. Very recently it has been shown that fragments of tau can discriminate between different sulfation modifications (6-*O*-sulfation) on heparin[19]. This work showed for the first time that, *in vitro*, tau can discriminate between very structurally similar glycans and that tau-HS binding was greatly affected by modifications at the 6-*O* position. Within the cell there are a variety of enzymes known to be important for imparting this information on cellular receptors, thus we envisioned that there might be a specific protein or motif that would allow specification of tau entry.

In this work we used central nervous system (CNS) cell lines, iPS-derived neurons, and mouse brain slice culture to understand the guidelines for tau uptake. We find that the quaternary structure of tau dictates the efficiency of uptake and we used tau monomers to screen for genetic modulators of internalization. We found that HSPG-modifying enzymes influence tau internalization and knockdown of these enzymes can repress the uptake of tau. We confirm that 6-*O*-sulfation patterns on HS chains are critical for tau binding, and show that competition or removal of these motifs on the cell surface reduced the internalization of tau.

Results

Internalization of tau in CNS culture is regulated by quaternary structure. Tau protein can form multiple quaternary structures in solution, and recent evidence suggests that small tau oligomeric species may play a critical role in the spread of tau pathology and neurotoxicity[12]. Furthermore, work on smaller fragments of tau have suggested that the size of tau can regulate seeding capacity[14]. Therefore, to study the overarching rules that govern the transmission of full length tau, we tested the uptake capacity of various tau structures in a variety of model systems, including human CNS-derived cell lines and iPS-derived neurons.

First, we recombinantly expressed and purified the longest isoform of tau, 2N4R, and used established protocols to produce oligomeric and fibrillized tau species (see Methods). Characterization of these constructs using non-reducing SDS-PAGE analysis, revealed that tau monomers appear as one distinct band at ~64 kDa, while tau oligomers/fibrils show additional bands of high molecular weight potentially corresponding to some sort of protofibril species (Fig. 1a). TEM preparations of fibril samples displayed characteristic long helical filaments

that could be fragmented upon sonication (Fig. 1a). We employed Dynamic Light Scattering (DLS) analysis to further characterize our tau constructs[20]. Analysis of our different tau species (Fig. 1b) showed, as expected, that monomeric tau was monodispersed and small in average size (5.7 ± 0.9 nm), whereas oligomers, sonicated fibrils and fibrils were larger and more dispersed (19 ± 3 nm, 33 ± 11 nm, and 80 ± 8 nm respectively).

To test the efficacy of these tau species towards internalization by cells, we labeled each protein preparation with an Alexa Fluor-488 (AF488) probe and then added various concentrations of protein to the cell media of H4 neuroglioma cells. After one hour, cells were washed, lifted from the plate and analyzed for fluorescence using flow cytometry. To control for non-specific binding to the membrane, identical experiments were performed at 4 °C (a non-permissive temperature for endocytosis), and any fluorescence observed was subtracted from our results. Monomeric, oligomeric and sonicated fibrils were efficiently internalized, while fibril samples were not (Fig. 1c and Supplementary Fig. 1d). Tau uptake was a time-dependent process, with uptake observed in as little as 10 minutes (Supplementary Fig. 1a). This assay for tau uptake was robust for other human CNS cell lines, including SHSY-5Y neuroblastoma, and ReN VM neural progenitors (Supplementary Fig. 1b,c). Further, human iPS-derived neurons also showed a preference for smaller structures of tau, with fibrillized tau showing nearly no uptake (Fig. 1d). Taken together, these results suggest that cellular uptake of tau is regulated by size and that large species of tau are inefficiently internalized across multiple cell types.

Functional genomics to find modulators of tau uptake. With a robust and high-throughput assay for tau uptake in hand, we used this platform to screen for genetic modulators that could either increase or decrease tau internalization. To do this, we developed an H4 CRISPRi cell line that stably expresses a catalytically inactive Cas9 fusion protein (dCas9-KRAB). CRISPRi represses transcription of genes with high specificity using single guide RNAs (sgRNAs) that guide the dCas9-KRAB protein to the transcription start site (TSS) of the targeted gene[21]. As a proof of concept, we screened a next-generation CRISPRi library of sgRNAs that targeted 3200 different genes with five different sgRNAs per gene, and contained hundreds of non-targeting negative-control sgRNAs[22]. H4 CRISPRi cells transduced with sgRNAs were then incubated with 25 nM AF488 labeled 2N4R monomer (2N4R-488) for 1 hr and sorted based on AF488 fluorescence. The cell populations with the top and bottom thirds of AF488 fluorescence, representing higher than average and lower than average tau uptake, respectively, were recovered, genomic DNA was isolated and the locus encoding the sgRNA was PCR-amplified and frequencies of each sgRNA in the two populations were determined by next-generation sequencing (Fig. 2a). To detect hit genes, we applied our previously developed quantitative framework for pooled genetic screens[23,24] as described in the Methods.

We selected sixteen genes for individual validation studies, including genes with particularly strong phenotypes in the primary screen, as well as genes in pathways previously implicated in tau uptake. Fifteen of the sixteen follow-up hits were found to repress expression of their target gene (i.e. knockdown) as determined by qPCR (Supplementary Fig. 2a). Fourteen of the fifteen gene knockdowns also reproduced their screen phenotype i.e. either increased or decreased tau uptake as compared to a non-targeting sgRNA control (Fig. 2b and Supplementary Fig. 2b).

Interestingly, we found that some of the strongest phenotypes in our screen were attributed to genes that are known cell cycle regulators (Supplementary Fig. 2c). The selective knockdown of genes such as TP53, led to a decrease in G1 length and thus an overall increase in cell proliferation (Supplementary Fig. 2d). Endocytosis is known to increase during G1 phase[25]; therefore, it seemed logical that cell cycle regulators that can shorten the G1 phase could reduce the amount of tau uptake and vice versa. In line with these observations a small molecule inhibitor of CDK4/6 that causes a stall in G1 phase (PD0332991) was sufficient to almost double the amount of tau taken up in H4 cells (Supplementary Fig. 2e). Further work will be needed to dissect if and how these genes might influence post-mitotic neurons.

Hits that were of particular interest included genes involved in heparan sulfate proteoglycan (HSPG) biosynthesis (EXT2 and HS6ST1) as well as DNM2, a GTPase involved in endocytosis. These single gene knockdowns repressed uptake of tau monomer by over 50% (Fig. 2b) and also reduced the uptake of tau oligomers (Fig. 2c). Further, these gene knockdowns were sufficient to reduce the uptake of tau in iPS-derived neurons (Fig. 2d). Treatment of cells with an inhibitor for DNM2, Dynasore, was also able to reduce uptake of tau (Supplementary Fig. 2 f).

Tau binds to heparin derivatives and shows specificity for 6-O-sulfated heparins. Based on our pilot screen results, we were particularly interested in the enzymes involved in HSPG biosynthesis. Previous reports had indicated that internalization of tau could be regulated by HSPGs[16], but our identification of HS6ST1, an enzyme that is responsible for 6-*O*-sulfation of HSPGs, supports a hypothesis that specific motifs on HSPGs might be important for tau uptake.

HSPGs are decorated with HS chains that consist of a repeating GlcA-GlcNAc building block. During assembly, HS chains can be highly modified and, importantly for their function, they can be sulfated at multiple sites within the disaccharide (Fig. 3a). To ascertain whether specific sulfation motifs were important for tau binding, we employed a heparin ELISA assay. In this assay, biotin-labeled heparin derivatives (Fig. 3b) were immobilized on streptavidin-coated plates, purified tau protein was incubated with the plate at increasing concentrations, and antibodies were used to detect tau binding. Tau bound heparin with an affinity of 4.6 ± 0.6 nM, consistent with previous reports[26]. Over sulfated heparin (>3 sulfates per disaccharide) bound tau even tighter (2.2 ± 0.5 nM), while fully-desulfated heparin showed a drastically reduced binding (>1 μM) (Fig. 3c). Removal of *N*-sulfates or 2-*O*-sulfates had little effect on tau binding (15.0 ± 5 nM and 7.4 ± 1.0 nM, respectively), while removal of all *O*-sulfates and, in particular 6-*O*-sulfates, led to a significant decrease in tau binding (>1 μM in each case; Fig. 3c,d). The relative binding of 6-*O*-desulfated heparin in the presence of 10 nM tau was 6.9% that of heparin, consistent with our hypothesis that tau interacts with the 6-*O*-sulfation motif on HS chains, and that HS is important for tau internalization.

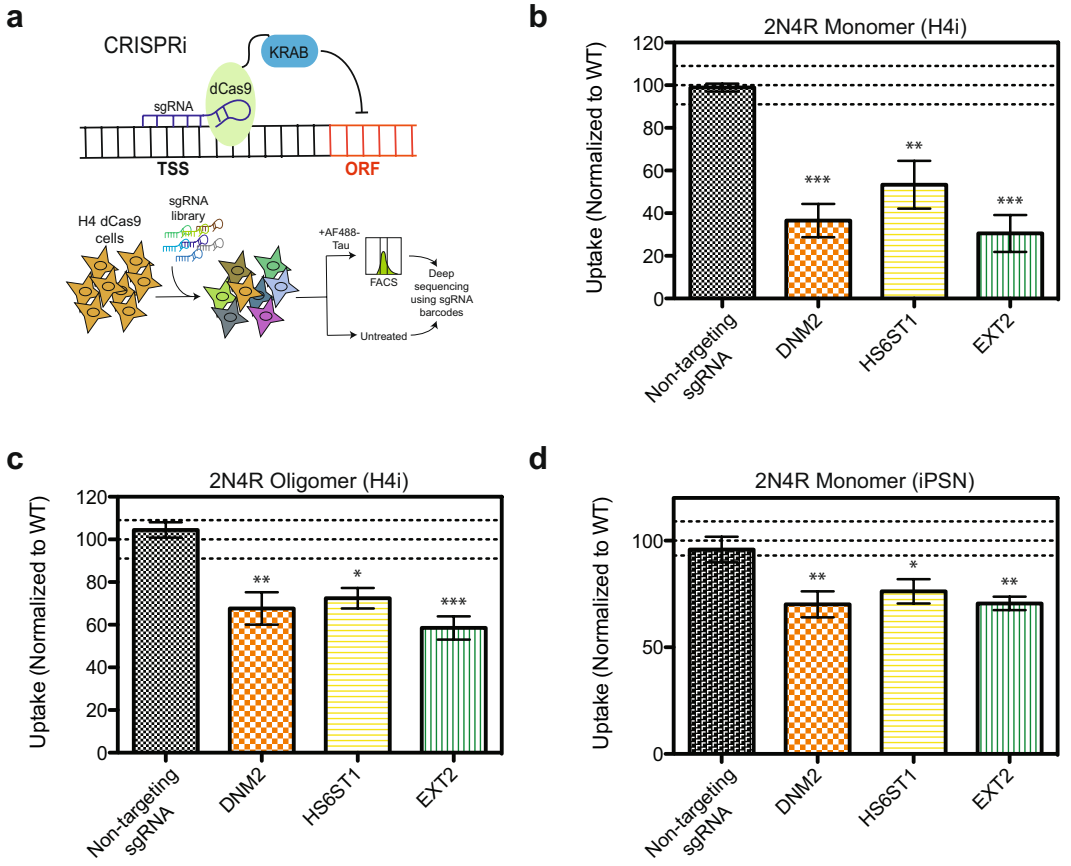

Figure 2. CRISPRi screen for tau uptake modulators. (**a**) Screening strategy using H4 CRISPRi cells, see text for details. (**b**) Reconfirmation of selected hits in H4i cells with 2N4R monomer (50 nM, 1 h at 37 °C), normalized to a WT (no sgRNA) control. (**c**) Uptake of 2N4R oligomers (50 nM, 1 h at 37 °C) in H4i cells with selected gene knockdowns, normalized to a WT (no sgRNA) control. (**d**) Uptake of 2N4R monomer (200 nM, 1 h at 37 °C) in iPS-derived neurons with selected gene knockdowns, normalized to a WT (no sgRNA) control. All uptake experiments were performed in duplicate over three independent experiments with the data combined. Lines on the graphs represent WT mean +/− 3 standard deviations, error bars represent SEM, a one-way ANOVA analysis with Dunnett's method was used to determine significance between the gene knockdown and the non-targeting sgRNA *p-value ≤ 0.05, **p-value ≤ 0.01, ***p-value ≤ 0.001.

Cellular internalization of tau is effected by the presence of 6-O-sulfation. To confirm that 6-*O*-sulfation was indeed a determinant of tau uptake, we developed a cellular competition experiment to monitor tau internalization. In this experiment, we added heparin or heparin derivatives free into the cell media immediately prior to addition of 2N4R-488. We found that internalization of tau can be efficiently competed by the presence of heparin or HS in the media (Fig. 4a). Likewise, addition of 2-*O*-desulfated heparin was able to reduce uptake, whereas 6-*O*-desulfated heparin or chondroitin sulfate (negative control) were significantly less effective at reducing uptake (Fig. 4a). These results were consistent when tested in iPS-derived neurons (Fig. 4b), demonstrating that the 6-*O*-sulfation motif is indeed a critical determinant for cellular tau entry.

To test if HS 6-*O*-sulfation would also prevent internalization of tau in an *ex vivo* system, we generated acute brain slices from adult mice using established methods[27]. These slices showed normal electrophysiology, suggesting good vitality (Supplementary Fig. 3a). Their ability to uptake tau was tested by incubating the cultures with 2N4R-488 for 30 min at 37 °C or, as a control, 4 °C. The cultures were washed, stained with Hoechst dye to label nuclei, and mounted on coverslips to image. Incubation at 37 °C showed uptake of tau in the slice cultures, whereas very little fluorescence was observed in the 4 °C control cultures (Fig. 4c and Supplementary Fig. 3b). Consistent with our previous results, incubation with heparin, heparan sulfate, or 2-*O*-desulfated heparin reduced uptake of tau as quantified by the median 488 fluorescence intensity (Fig. 4d). Chondroitin sulfate and 6-*O*-desulfated heparin incubation did not reduce the median fluorescence, verifying that 6-*O*-sulfation is also important for tau internalization *ex vivo* (Fig. 4d and Supplementary Fig. 3b). Quantification of median Hoechst fluorescence across all the images showed that similar cell numbers were analyzed for each condition (Supplementary Fig. 3c).

Finally, in order to test if direct removal of 6-*O*-sulfates from the cell surface could reduce uptake of tau in cell culture, we overexpressed two different extracellular endosulfatases (Sulf1 & Sulf2) that selectively cleave 6-*O*-sulfates on GlcNAc[28]. Overexpression of these enzymes in H4 cells, showed a dramatic decrease in tau uptake

a

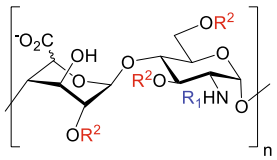

Heparan Sulfate/Heparin

R^1 = H, Ac, or SO_3^-

R^2 = H or SO_3^-

b

GAG	MW	Description
Heparin	19 kDa	>70%: Ido(2S)-GlcNS(6S)
Over sulfated Heparin	12-13 kDa	>3/5 sulfates per disaccharide
Fully desulfated Heparin	12-13 kDa	Degree of desulfation>90%
N-desulfated Heparin	11-12 kDa	Degree of de-*N*-sulfation>90%
O-desulfated Heparin	11-12 kDa	Degree of de-*O*-sulfation>90%
6-*O*-desulfated Heparin	11-12 kDa	Degree of de-6*O*-sulfation>90%; degree of de-2 *O*-sulfation <20%
2-*O*-desulfated Heparin	12-13 kDa	Degree of de-2*O*/3*O*-sulfation>90%; degree of de-6 *O*-sulfation <10%

c

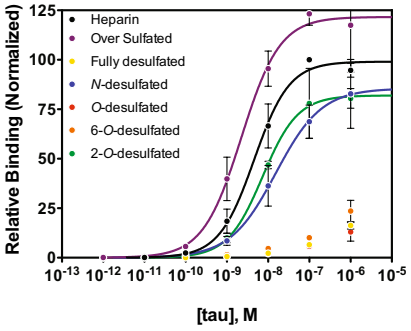

d

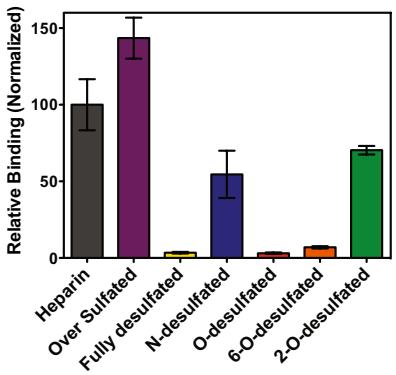

Figure 3. Binding of tau to heparin derivatives. (**a**) HS chains consist of GlcA/IdoA-GlcNAc disaccharide units that can be modified at positions indicated in red and blue. (**b**) List of heparin/heparin derivatives that were used, their average molecular weights, and description of their sulfation modifications. (**c**) Binding of 2N4R to various heparin derivatives by ELISA with data fit to a Hill binding model (line) where appropriate. (**d**) Normalized relative binding of 2N4R (10 nM) to various heparin derivatives. Three independent experiments were performed, data were normalized to heparin controls, and the error shown is SD.

with Sulf1 reducing uptake to 17 ± 9%, and Sulf2 reducing uptake to 36 ± 15% (Fig. 4e). Overexpression of the constructs was confirmed with immunocytochemistry and qPCR analysis (Fig. 4f and Supplementary Fig. 3d) and the ability of the enzymes to reduce 6-*O* sulfation on the cell surface was confirmed by HPLC (Supplementary Fig. 3e,f).

Discussion

In recent years, a growing body of literature has reinforced the hypothesis that prion-like cell-to-cell propagation of protein aggregates underlies disease progression of numerous neurodegenerative disorders[29]. For some of these protein aggregates (PrP, α-synuclein), specific pathways and protein conformers that are key for transmission have been delineated quite fully[15,30]. However for other proteins, such as tau, many details regarding its transmissibility are still unclear. It has been shown in various cellular and animal models that exogenously added tau aggregates can induce tau pathology;[9,13] however, the disparity between the experimental systems and the tau species used in each study makes it hard to draw a unifying theme. Tau is a complex protein that has several isoforms, posttranslational modifications, and the ability to form multiple quaternary structures[31]. Therefore, we have focused our research on the development of a cellular assay that can robustly detect internalization across various tau constructs and CNS cell systems.

The data presented here demonstrate that full-length human tau (2N4R) can be efficiently internalized across multiple relevant cell systems and that this uptake is dependent on the overall size of the tau species, similar to what has been seen before for smaller fragments of tau[14]. By screening through thousands of potential gene regulators, we have identified enzymes involved in HSPG synthesis/modification as critical modulators of tau internalization. This is a critical point, since it is still debated exactly how tau induces neurotoxicity. One hypothesis suggests that tau oligomers are the toxic species and that the formation of tau fibrils inside neurons (NFTs) could be a protective mechanism. This is supported by neuropathological studies measuring oligomeric tau (MC1+) in AD patients which show that neuronal loss and cognitive deficits correlate with increased MC1 reactivity and that these changes precede NFT formation[32]. Our data are consistent with this hypothesis, as tau fibrils were unable to be internalized, and thus would be unable to "seed" misfolding inside the cell. Our results also indicate that both monomeric and oligomeric tau are internalized with similar efficiency and presumably using similar cellular mechanisms, since genetic regulators of monomer tau uptake also affect oligomer uptake. However, this work has only focused on uptake mechanism of "naked" tau and has not focused on seeding potential or the possibility of exosome transfer of fibrils between neurons[33]. But, as tau oligomers and monomers have been found elevated in

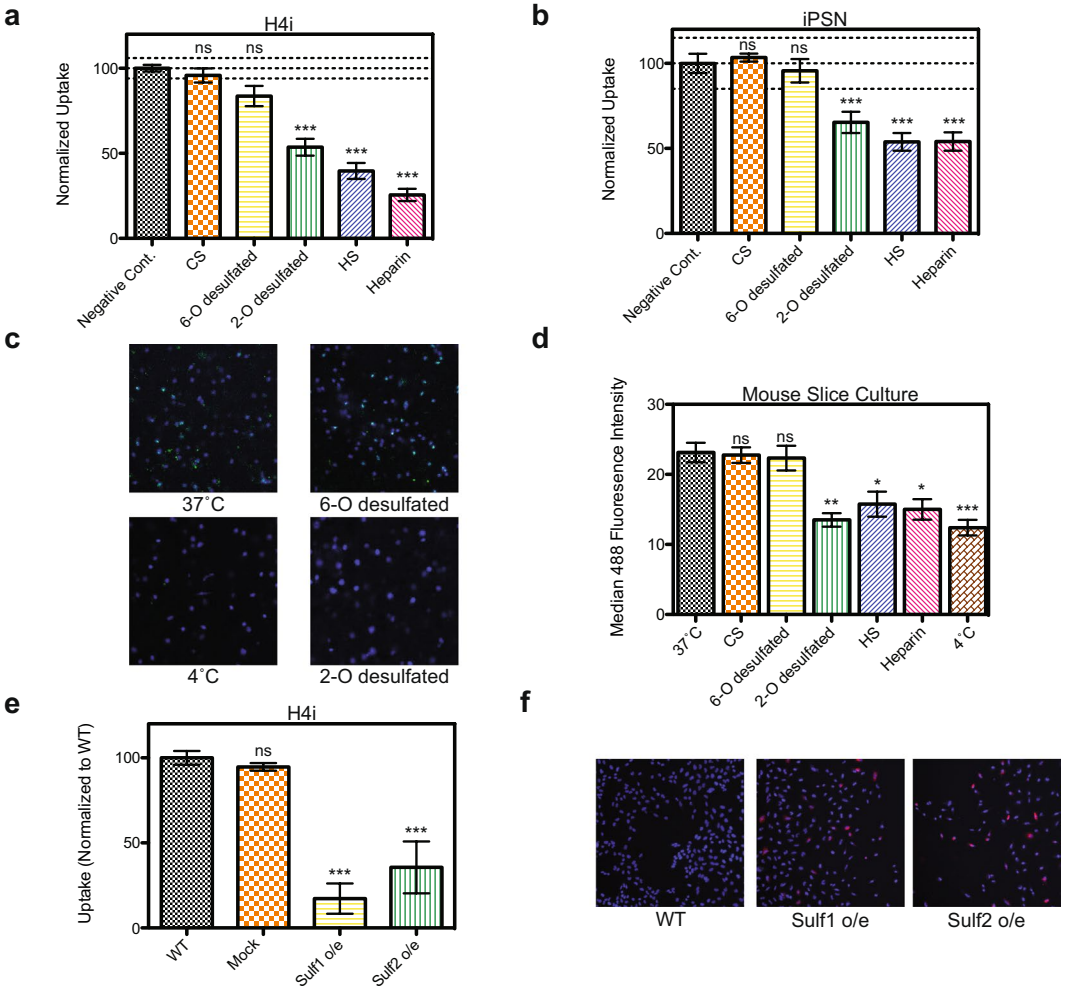

Figure 4. 6-O sulfation regulates tau uptake in CNS culture. (**a**) Internalization of 2N4R-488 (50 nM, 1 h at 37 °C) into H4 cells is strongly inhibited by incubation with heparin, heparan sulfate, and 2-*O*-desulfated heparin as compared to 6-*O*-desulfated heparin or chondroitin sulfate (0.05 mg/ml for all derivatives). (**b**) Internalization of 2N4R-488 (200 nM, 1 h at 37 °C) into iPS-derived neurons is inhibited by incubation with heparin, heparan sulfate, and 2-*O*-desulfated heparin as compared to 6-*O*-desulfated heparin or chondroitin sulfate (0.5 mg/ml for all derivatives). All uptake experiments were performed in duplicate over three independent experiments with the data combined. Lines on the graphs represent WT mean +/− 3 standard deviations, error bars represent SEM, and a one-way ANOVA analysis with Dunnett's method was used to determine significance compared to the negative control *p-value ≤ 0.05, **p-value ≤ 0.01, ***p-value ≤ 0.001, ns = not significant. (**c**) Internalization of 2N4R-488 (200 nM, 30 min at 37 °C) into mouse slice culture is strongly inhibited by incubation with 2-*O*-desulfated heparin, but not 6-*O*-desulfated heparin (0.5 mg/ml). Hoechst stain is used to label nuclei. (**d**) Quantification of the median 488 fluorescence intensity for tau uptake in mouse slice culture. Two independent experiments were performed with multiple images (>5) from each condition. Error bars represent SEM. (**e**) Uptake of 2N4R-488 (50 nM, 1 h at 37 °C) tau is reduced when Sulf1 or Sulf2 is overexpressed in H4 cells as compared to WT or mock transfected cells. Uptake experiments were performed in duplicate over three independent experiments with the data normalized to WT and combined. Error bars represent SEM. (**f**) ICC confirms that Sulf1 and Sulf2 are overexpressed (red) in H4 cells. Hoechst stain is used to label nuclei.

the CSF of AD patients[34,35] and tau antibodies have been shown to block tau spreading[36,37] it seems likely our assay recapitulates at least one *in vivo* scenario.

Using CRISPRi technology, we identified multiple genetic factors that can influence the uptake of tau in cell culture. The identification of HSPGs as regulators of tau internalization is not an entirely new concept. Indeed, it has been known for years that tau can bind heparin, and that this molecule can be used as an *in vitro* inducer of aggregation[38]. Tau internalization has also been linked to HSPGs previously[16], and the data presented here adds more detail to the molecular picture and confirms previous *in vitro* work that identified 6-*O* sulfation as a major determinant of tau binding[19]. The HSPG family consists of over 12 members, with a wide array of HS sulfation modifications and chain length complexity. Our comprehensive analysis has shown that binding of tau to HS in a cellular context is directly related to the sulfation pattern, and specifically on the presence of 6-*O* sulfates on the

glucosamine subunit. Further work will be needed to understand if there are specific HS chain lengths or regions on tau that are important for this interaction.

This work is an important step forward in the characterization of HS-tau interactions. With these new insights we can begin to envision ways to design small molecules that mimic the HS structures that interact with tau to block its aggregation and neutralize its toxicity. It is plausible to expect that novel treatments that target the HS-tau interaction may contribute to AD treatment and could improve the effects of other treatments.

Methods

Chemicals. Heparin, chondroitin sulfate, heparan sulfate, and desulfated heparins (Neoparin & Galen Labs Supplies). Dynasore hydrate (Sigma). Hoechst (Thermo Scientific).

Protein purification, labeling and fibrillization. Full length tau protein (2N4R, 1-441aa) was purified with slight modification to previously published protocols[39]. Briefly, 2N4R tau in the pRK172 plasmid was expressed in *E. coli* BL21 (DE3). Cell pellets were harvested and resuspended in cell lysis buffer (50 mM MES pH 6.5, 5 mM DTT, 1 mM PMSF, 1 mM EGTA) + cOmplete protease inhibitor tablets (Roche). Lysate was sonicated, boiled for 10 min, and then centrifuged at 50,000 × g for 30 min at 4 °C. The supernatant was then precipitated with ammonium sulfate (20% w/v) and centrifuged at 20,000 × g for 30 min at 4 °C. The pellet was resuspended into 4 mL of MonoS Buffer A (50 mM MES pH 6.5, 50 mM NaCl, 2 mM DTT, 1 mM PMSF, 1 mM EGTA) and dialyzed overnight against the same buffer. The protein was loaded onto a MonoS column (GE Healthcare) and eluted with a linear gradient of NaCl using MonoS Buffer B (Buffer A + 1 M NaCl). Fractions containing 2N4R tau were pooled, concentrated, and dialyzed overnight into PBS pH 7.4. Protein concentration was determined using a BCA assay (Thermo Scientific).

Protein was labeled with Alexa Fluor® 488 or 647 5-SDP ester (Life Technologies) according to the suppliers instructions. After labeling, 100 mM glycine was added to quench the reaction and the proteins were subjected to Zeba desalting columns (Thermo Scientific) to remove any unreacted label. Average label incorporation was between 1 and 1.5 moles/mole of protein, as determined by measuring fluorescence and protein concentration (A_{max} x MW of protein/[protein] x ε_{dye}). To prepare tau fibrils and oligomers, 10 uM protein, in PBS 1 mM DTT pH 7.4, was mixed with heparin (0.05 mg/ml) and incubated with shaking at 37 °C. The formation of oligomers was observed after 4 h of shaking, whereas fibril formation was formed after 5 days[13]. To make sonicated fibril samples, fibrillized protein was sonicated using a MiSonix Sonicator 4000 (QSonica, LLC) at 50% amplitude for 60 1 s pulses. Mutation of 2N4R (C291S, C322S) to remove both cysteine residues important for dimer formation allowed us to further confirm that tau monomer could indeed be internalized (data not shown).

Transmission electron microscopy. Tau fibrils and sonicated fibrils (1 μM) were absorbed on 200-mesh formvar-coated copper grids, washed, and stained with a 2% uranyl acetate solution. Grids were then imaged with a JEOL JEM-1230 (JEOL USA, Inc) at the indicated magnifications.

Dynamic light scattering. Protein solutions (1 μM) were filtered (0.45 μm) and analyzed using a Zetasizer Nano ZS (Malvern). The time-dependent autocorrelation function of the photocurrent at a fixed angle of 175° was acquired every 10 s, with 15–20 acquisitions for each run and with at least three repetitions. The error bars displayed on the DLS graphs were obtained by the standard deviation (SD) between replicates.

Cell culture, transfections and treatments. H4 cells were cultured in DMEM supplemented with 10% FBS, 100 μg/ml penicillin/streptomycin. SHSY-5Y cells were cultured in DMEM/F12 supplemented with 10% FBS, 100 μg/ml penicillin/streptomycin. ReN-VM cells were cultured on Matrigel (Corning) coated plates in DMEM/F12 supplemented with 2 μg/ml heparin (STEMCELL Technologies), 2% B27 (Life Technologies, 100 μg/ml penicillin/streptomycin, 20 μg/ml bFGF (Stemgent), 20 μg/ml EGF (Sigma). Cultures were maintained in a humidified atmosphere of 5% CO_2 at 37 °C. Transfection of H4 cells with Sulf1 (Addgene #13003) or Sulf2 (Addgene #13004) were performed with Lipofectamine 3000 (Invitrogen) according to the manufacturers instructions and cells were assayed 48 h later. Overexpression was confirmed with immunocytochemistry using the his tag epitope and qPCR. For competition experiments, heparin (and various derivatives) was added to the media just prior to tau addition at the indicated concentrations.

iPS culturing and differentiation. CRISPRi iPSc with an inducible TRE3G-dCas9KRAB-T2A-mCherry were maintained in 6-well Matrigel (Corning) coated plates with mTeSR1 media (STEMCELL Technologies) and split with ReLeSR (STEMCELL Technologies) at a 1:20 ratio every 4–5 days. For differentiation, CRISPRi cells were split with Accutase and virally infected twice with a NeuroD1-IRES-eGFP-Puro (Addgene #45567) according to previously published methods[40]. Doxycyclin was added to induce expression of NeuroD1, and the following day cells were selected with puromycin (5 μg/ml). After selection, cells were lifted with Accutase treatment and replated 1:12 in PEI coated 24-well plates. Three days later, media was changed to Brain Phys Neuronal Medium (STEMCELL Technologies) with doxycycline and AraC to remove any remaining dividing cells. At day 8, cells were infected with specific sgRNA constructs. iPS neurons were assayed between days 14–18 of maturity as described below. Immunocytochemistry was used to confirm neuronal properties (Supplementary Fig. 1e).

Flow cytometry. H4 cells were plated at 50,000 cells per well in a 24-well plate. The next day media was replaced, and cells were treated with varying concentrations of AF488-labeled tau protein for 1 h (unless indicated otherwise) at 37 °C. For ReN-VM uptake experiments the media was replaced with DMEM/F12 without B27 or heparin. Cells were then washed twice with PBS and trypsinized to lift cells from the plate. Identical control experiments were performed at 4 °C to confirm that tau protein was internalized and not just adhering to the cell membrane. Lifted cells were analyzed using an Accuri-C6 Flow Cytometer and propidium iodide was used to exclude dead cells from the analysis.

CRISPRi screen. We generated a stable CRISPRi-enabled H4 neuroglioma cell line by transducing H4 cells with the lentiviral plasmid pHR-SFFV-dCas9-BFP-KRAB[41] and selecting a polyclonal population of BFP-expressing cells by FACS. These cells were transduced with a next-generation CRISPRi sgRNA library (sublibrary "Cancer and Apoptosis")[22], and transduced cells were selected using puromycin (1 μg/mL). Media was replaced with fresh DMEM containing AF488-labeled Tau monomers at a final concentration of 25 nM for 1 h at 37 °C. Cells were washed twice, trypsinized, and resuspended in FACS buffer (PBS with 0.5% FBS). A BD-FACAria II, was used to sort live cells into two populations based on the top and bottom thirds of AF488 fluorescence; approximately 15 million and 17 million cells were recovered from the high- and low-fluorescence populations, respectively. The resulting DNA was isolated, the cassette encoding the sgRNA was amplified by PCR, and relative sgRNA abundance was determined by next-generation sequencing as previously described[21,24]. We analyzed the resulting data using our previously developed quantitative framework for pooled genetic screens[23,24]. Statistical significance for each targeted transcription start site was calculated using the Mann-Whitney U test to compare the phenotypes of the 5 sgRNAs targeting the transcription start site to the phenotype distribution of the 280 non-targeting sgRNAs in the library.

ELISA. Heparin was purchased from AMSBio (AMS.HEP001-100) and all heparin derivatives were purchased from Neoparin (GT6011, GT6012, GT6013, GT6014, GT6020, GT6030). Heparin/heparin derivatives were biotinylated by reacting their free amines (estimated abundance of 1–5% for heparin) with EZ-link Sulfo-NHS-LC-Biotin (Thermo) according to the manufacturer's protocol. Briefly, heparin/heparin derivatives and biotin reagent were combined in PBS (pH 7.4) and incubated at room temperature for 1 h. Excess reagent was removed, buffer exchanged for Milli-Q water, and samples concentrated by centrifugation with Amicon Ultra-0.5 mL Centrifugal Filters (Millipore, 3k cut-off). For ELISA assays, biotinylated heparin/heparin derivatives were immobilized on streptavidin plates followed by a 2 h incubation with 2N4R tau protein containing a C-terminal myc tag (10-fold dilution series). Bound tau was detected using an anti-myc HRP-conjugated antibody (Bethyl, A190-105P), visualized using TMB substrate (R&D Systems), and quantified by UV-Vis. Absorbance for each plate was measured at 450 and 550 nm. The 550 nm measurement is a correction for plate imperfections and was subtracted from the 450 nm values. Data were normalized to heparin controls and fit with a Hill binding mathematical model where appropriate using the equation $Y = B_{max} * X^H / (K_d{}^H + X^H)$, where H is the Hill slope (variable), X is the concentration of tau, and B_{max} is the binding maximum.

Mouse slice culture & EPSP measurements. Protocols and procedures were approved by the Institutional Animal Care and Use Committee of the University of California, Santa Barbara and were performed according to the Guide for the Care and Use of Laboratory Animals of the National Institutes of Health. Slice cultures were prepared as previously described[27]. Hippocampal excitatory postsynaptic potentials (EPSPs) were measured using a multi-electrode array (MEA). Stimulus current was injected into a region of the hippocampal slice by an MEA electrode, with the magnitude of stimulus current ranging from 20–80 μA. EPSPs were then measured by recording an electrode in a different region of the hippocampal slice. Smaller stimulus currents excite fewer cells, and thus the measured EPSPs have smaller magnitudes.

qPCR. Purelink RNA Extraction Kit (Invitrogen) was used to isolate RNA from samples. RNA (1 μg) was then converted to cDNA using SuperScript Reverse Transcriptase III (Invitrogen) according to the supplier's instructions. Real-time quantitative PCR was performed using Power SYBR Green PCR Master Mix (Applied Biosystems) according to QuantStudioTM 12 K Flex Real-Time PCR System protocol. GAPDH mRNA level was used to normalize samples.

Immunocytochemistry. Cells were fixed with 4% paraformaldehyde for 15 min at RT followed by three washes with PBS. Cells were permeabilized with 0.25% Triton X-100 in PBS, and blocked for 1 hr in blocking buffer at RT (1% BSA, 300 mM Glycine, 0.1% Gelatin, 4% Donkey Serum in TBST). After blocking, cells were incubated with primary antibodies diluted in blocking buffer overnight at 4 °C. The day after cells were washed three times (5 min each) with 0.05% Tween-20 in PBS. The following primary antibodies were used: Tau-46 (Invitrogen, 36400, 1:1000), MAP2 (Millipore, AB5622, 1:1000), and anti-his (Thermo Scientific, MA1-21315, 1:1000). Secondary antibodies (Life Technologies, A21422, A21206, 1:1000) were incubated for 1 hr at RT, washed three times with 0.05% Tween-20 in PBS and imaged with an Olympus IX71 Microscope or an Olympus Fluoview 1000 Spectral Confocal.

Disaccharide analysis. Cells pellets of WT, Sulf1, and Sulf2 overexpressing cells were resuspended in PBS and digested with pronase (final concentration 2 mg/mL) overnight at 37 °C. Samples were passed through a 0.22-μm syringe filter to remove cell particulates and applied to DEAE-cellulose columns equilibrated with 0.2 M NaCl in PBS. The columns were extensively washed with 0.2 M NaCl in PBS, the GAGs eluted with 1.0 M NaCl in PBS, and the eluted fractions combined, flash-frozen and lyophilized. Purified GAGs were digested using a combination of heparinases I, II, and III, and the resultant disaccharides were isolated by size filtration and subsequently labeled with AMAC, as previously described[42]. AMAC-labeled HS was lyophilized and reconstituted in 50% DMSO and stored at −20 °C prior to analysis.

Sample analysis was performed on a Zorbax Eclipse XDB-C18 RP-HPLC column (4.6 mm × 75 mm, 3.6 mm; Agilent Technologies) running on an Agilent 1100 Series HPLC system. Samples were diluted with 60 mM ammonium acetate (pH 5.6) and applied to the column, which was equilibrated in 98% solution A/2% solution B (A: 60 mM ammonium acetate, pH 5.6; B: acetonitrile). The column was held at 2% solution for 0.5 min, and the AMAC-labeled disaccharides were then eluted over a shallow gradient of 2–12% solution B over 25 min at a flow rate of 1 mL/min. Disaccharides were detected in-line by UV-Vis (260 nm). The column was regenerated

with 95% solution B prior to equilibration. To confirm peak identities, eight standards purchased from Iduron (ΔUA2S – GlcNS6S, HD001; ΔUA2S – GlcNS, HD002; ΔUA2S – GlcNAc6S, HD003; ΔUA – GlcNS6S, HD004; ΔUA – GlcNS, HD005; ΔUA – GlcNAc, HD006; ΔUA2S – GlcNAc, HD007; ΔUA – GlcNAc6S, HD008) were labeled with AMAC and spiked into cell-derived samples.

References

1. Brandt, R., Hundelt, M. & Shahani, N. Tau alteration and neuronal degeneration in tauopathies: mechanisms and models. *Biochim Biophys Acta* **1739**, 331–354, https://doi.org/10.1016/j.bbadis.2004.06.018 (2005).
2. Jeganathan, S., von Bergen, M., Mandelkow, E. M. & Mandelkow, E. The natively unfolded character of tau and its aggregation to Alzheimer-like paired helical filaments. *Biochemistry* **47**, 10526–10539, https://doi.org/10.1021/bi800783d (2008).
3. Schweers, O., Schonbrunn-Hanebeck, E., Marx, A. & Mandelkow, E. Structural studies of tau protein and Alzheimer paired helical filaments show no evidence for beta-structure. *J Biol Chem* **269**, 24290–24297 (1994).
4. Hyman, B. T., Van Hoesen, G. W., Damasio, A. R. & Barnes, C. L. Alzheimer's disease: cell-specific pathology isolates the hippocampal formation. *Science* **225**, 1168–1170 (1984).
5. Braak, H. & Braak, E. Neuropathological stageing of Alzheimer-related changes. *Acta neuropathologica* **82**, 239–259 (1991).
6. Desplats, P. *et al*. Inclusion formation and neuronal cell death through neuron-to-neuron transmission of alpha-synuclein. *Proceedings of the National Academy of Sciences of the United States of America* **106**, 13010–13015, https://doi.org/10.1073/pnas.0903691106 (2009).
7. Pearce, M. M., Spartz, E. J., Hong, W., Luo, L. & Kopito, R. R. Prion-like transmission of neuronal huntingtin aggregates to phagocytic glia in the Drosophila brain. *Nature communications* **6**, 6768, https://doi.org/10.1038/ncomms7768 (2015).
8. Munch, C., O'Brien, J. & Bertolotti, A. Prion-like propagation of mutant superoxide dismutase-1 misfolding in neuronal cells. *Proceedings of the National Academy of Sciences of the United States of America* **108**, 3548–3553, https://doi.org/10.1073/pnas.1017275108 (2011).
9. Clavaguera, F. *et al*. Transmission and spreading of tauopathy in transgenic mouse brain. *Nature cell biology* **11**, 909–913, https://doi.org/10.1038/ncb1901 (2009).
10. Takeda, S. *et al*. Neuronal uptake and propagation of a rare phosphorylated high-molecular-weight tau derived from Alzheimer's disease brain. *Nature communications* **6**, 8490, https://doi.org/10.1038/ncomms9490 (2015).
11. Lasagna-Reeves, C. A. *et al*. Alzheimer brain-derived tau oligomers propagate pathology from endogenous tau. *Scientific reports* **2**, 700, https://doi.org/10.1038/srep00700 (2012).
12. Lasagna-Reeves, C. A. *et al*. Tau oligomers impair memory and induce synaptic and mitochondrial dysfunction in wild-type mice. *Molecular neurodegeneration* **6**, 39, https://doi.org/10.1186/1750-1326-6-39 (2011).
13. Usenovic, M. *et al*. Internalized Tau Oligomers Cause Neurodegeneration by Inducing Accumulation of Pathogenic Tau in Human Neurons Derived from Induced Pluripotent Stem Cells. *The Journal of neuroscience: the official journal of the Society for Neuroscience* **35**, 14234–14250, https://doi.org/10.1523/JNEUROSCI.1523-15.2015 (2015).
14. Mirbaha, H., Holmes, B. B., Sanders, D. W., Bieschke, J. & Diamond, M. I. Tau Trimers Are the Minimal Propagation Unit Spontaneously Internalized to Seed Intracellular Aggregation. *J Biol Chem* **290**, 14893–14903, https://doi.org/10.1074/jbc.M115.652693 (2015).
15. Mao, X. *et al*. Pathological alpha-synuclein transmission initiated by binding lymphocyte-activation gene 3. *Science* **353**, https://doi.org/10.1126/science.aah3374 (2016).
16. Holmes, B. B. *et al*. Heparan sulfate proteoglycans mediate internalization and propagation of specific proteopathic seeds. *Proceedings of the National Academy of Sciences of the United States of America* **110**, E3138–3147, https://doi.org/10.1073/pnas.1301440110 (2013).
17. Xu, D. & Esko, J. D. Demystifying heparan sulfate-protein interactions. *Annual review of biochemistry* **83**, 129–157, https://doi.org/10.1146/annurev-biochem-060713-035314 (2014).
18. Kreuger, J. & Kjellen, L. Heparan sulfate biosynthesis: regulation and variability. *The journal of histochemistry and cytochemistry: official journal of the Histochemistry Society* **60**, 898–907, https://doi.org/10.1369/0022155412464972 (2012).
19. Zhao, J. *et al*. Glycan Determinants of Heparin-Tau Interaction. *Biophysical journal* **112**, 921–932, https://doi.org/10.1016/j.bpj.2017.01.024 (2017).
20. Minton, A. P. Recent applications of light scattering measurement in the biological and biopharmaceutical sciences. *Analytical biochemistry* **501**, 4–22, https://doi.org/10.1016/j.ab.2016.02.007 (2016).
21. Gilbert, L. A. *et al*. Genome-Scale CRISPR-Mediated Control of Gene Repression and Activation. *Cell* **159**, 647–661, https://doi.org/10.1016/j.cell.2014.09.029 (2014).
22. Horlbeck, M. A. *et al*. Compact and highly active next-generation libraries for CRISPR-mediated gene repression and activation. *eLife* **5**, https://doi.org/10.7554/eLife.19760 (2016).
23. Kampmann, M., Bassik, M. C. & Weissman, J. S. Integrated platform for genome-wide screening and construction of high-density genetic interaction maps in mammalian cells. *Proceedings of the National Academy of Sciences of the United States of America* **110**, E2317–2326, https://doi.org/10.1073/pnas.1307002110 (2013).
24. Kampmann, M., Bassik, M. C. & Weissman, J. S. Functional genomics platform for pooled screening and generation of mammalian genetic interaction maps. *Nature protocols* **9**, 1825–1847, https://doi.org/10.1038/nprot.2014.103 (2014).
25. Quintart, J., Leroy-Houyet, M. A., Trouet, A. & Baudhuin, P. Endocytosis and chloroquine accumulation during the cell cycle of hepatoma cells in culture. *The Journal of cell biology* **82**, 644–653 (1979).
26. Elbaum-Garfinkle, S. & Rhoades, E. Identification of an aggregation-prone structure of tau. *Journal of the American Chemical Society* **134**, 16607–16613, https://doi.org/10.1021/ja305206m (2012).
27. Chong, S. A. *et al*. Synaptic dysfunction in hippocampus of transgenic mouse models of Alzheimer's disease: a multi-electrode array study. *Neurobiology of disease* **44**, 284–291, https://doi.org/10.1016/j.nbd.2011.07.006 (2011).
28. Morimoto-Tomita, M., Uchimura, K., Werb, Z., Hemmerich, S. & Rosen, S. D. Cloning and characterization of two extracellular heparin-degrading endosulfatases in mice and humans. *J Biol Chem* **277**, 49175–49185, https://doi.org/10.1074/jbc.M205131200 (2002).
29. Brettschneider, J., Del Tredici, K., Lee, V. M. & Trojanowski, J. Q. Spreading of pathology in neurodegenerative diseases: a focus on human studies. *Nature reviews. Neuroscience* **16**, 109–120, https://doi.org/10.1038/nrn3887 (2015).
30. Aguzzi, A., Sigurdson, C. & Heikenwaelder, M. Molecular mechanisms of prion pathogenesis. *Annual review of pathology* **3**, 11–40, https://doi.org/10.1146/annurev.pathmechdis.3.121806.154326 (2008).
31. Wang, Y. & Mandelkow, E. Tau in physiology and pathology. *Nature reviews. Neuroscience* **17**, 5–21, https://doi.org/10.1038/nrn.2015.1 (2016).
32. Haroutunian, V., Davies, P., Vianna, C., Buxbaum, J. D. & Purohit, D. P. Tau protein abnormalities associated with the progression of alzheimer disease type dementia. *Neurobiology of aging* **28**, 1–7, https://doi.org/10.1016/j.neurobiolaging.2005.11.001 (2007).
33. Wang, Y. *et al*. The release and trans-synaptic transmission of Tau via exosomes. *Molecular neurodegeneration* **12**, 5, https://doi.org/10.1186/s13024-016-0143-y (2017).
34. Sengupta, U. *et al*. Tau oligomers in cerebrospinal fluid in Alzheimer's disease. *Annals of clinical and translational neurology* **4**, 226–235, https://doi.org/10.1002/acn3.382 (2017).

35. Russell, C. L. *et al.* Comprehensive Quantitative Profiling of Tau and Phosphorylated Tau Peptides in Cerebrospinal Fluid by Mass Spectrometry Provides New Biomarker Candidates. *Journal of Alzheimer's disease: JAD* **55**, 303–313, https://doi.org/10.3233/JAD-160633 (2017).
36. Nobuhara, C. K. *et al.* Tau Antibody Targeting Pathological Species Blocks Neuronal Uptake and Interneuron Propagation of Tau *in Vitro*. *The American journal of pathology* **187**, 1399–1412, https://doi.org/10.1016/j.ajpath.2017.01.022 (2017).
37. Lee, S. H. *et al.* Antibody-Mediated Targeting of Tau *In Vivo* Does Not Require Effector Function and Microglial Engagement. *Cell reports* **16**, 1690–1700, https://doi.org/10.1016/j.celrep.2016.06.099 (2016).
38. Goedert, M. *et al.* Assembly of microtubule-associated protein tau into Alzheimer-like filaments induced by sulphated glycosaminoglycans. *Nature* **383**, 550–553, https://doi.org/10.1038/383550a0 (1996).
39. Mulot, S. F., Hughes, K., Woodgett, J. R., Anderton, B. H. & Hanger, D. P. PHF-tau from Alzheimer's brain comprises four species on SDS-PAGE which can be mimicked by *in vitro* phosphorylation of human brain tau by glycogen synthase kinase-3 beta. *FEBS letters* **349**, 359–364 (1994).
40. Zhang, Y. *et al.* Rapid single-step induction of functional neurons from human pluripotent stem cells. *Neuron* **78**, 785–798, https://doi.org/10.1016/j.neuron.2013.05.029 (2013).
41. Gilbert, L. A. *et al.* CRISPR-mediated modular RNA-guided regulation of transcription in eukaryotes. *Cell* **154**, 442–451, https://doi.org/10.1016/j.cell.2013.06.044 (2013).
42. Volpi, N. *et al.* Analysis of glycosaminoglycan-derived, precolumn, 2-aminoacridone-labeled disaccharides with LC-fluorescence and LC-MS detection. *Nature Protocols* **3**, 541–58, https://doi.org/10.1038/nprot.2014.026 (2014).

Acknowledgements

We thank Jason Gestwicki (UCSF) for the 2N4R pRK172 plasmid, Bruce Conklin (UCSF) for the CRISPRi iPS cells, the UCSB NRI-MCDB Microscopy Facility for use of the TEM and Confocal Microscope, the UCSB Stem Cell Core for use of the facility, and the UCSB BNL for access to the DLS. J.J.C. was supported by a postdoctoral fellowship from the Alzheimer's Association and the QB3/Calico Longevity Fellowship. S.K.S. was supported by a National Defense Science & Engineering Graduate (NDSEG) Fellowship. A.W.S. was supported by an NIH Training Grant (NIH/NRSA 5T32 GM007616-38). L.C.H.-W. was supported by an NIH/NIGMS grant (R01 GM093627). Support also came from an NIH Director's New Innovator Award (NIH/NIGMS DP2 GM119139) (M.K.), an Allen Distinguished Investigator Award (Paul G. Allen Family Foundation) (M.K.), the Tau Center Without Walls (NIH/NINDS U54 NS100717) (M.K., K.S.K), the Tau Consortium (K.S.K.) the Chan-Zuckerberg Biohub (M.K.) and the Paul F. Glenn Center for Aging Research (M.K.).

Author Contributions

J.N.R., J.J.C., A.W.S., G.M.M., and T.S. performed experiments and interpreted results. S.K.S. made and validated the H4 CRISPRi cell line. L.C.H.-W., M.K., and K.S.K., interpreted results and directed the research. J.N.R., J.J.C., L.C.H.-W., M.K., and K.S.K. wrote the manuscript.

Additional Information

Supplementary information accompanies this paper at https://doi.org/10.1038/s41598-018-24904-z.

Competing Interests: K.S.K. serves as a consultant and has shares in ADRx, serves as co-director of the Tau Consortium and is on the scientific advisory board of Cohen Veterans Bioscience. The remaining authors declare that they have no competing interests.

Publisher's note: Springer Nature remains neutral with regard to jurisdictional claims in published maps and institutional affiliations.